Frequency Regulation for Power System Dynamics with Variable and Low Inertia due to Renewable Energy

Patricia Hidalgo-Gonzalez

Frequency Regulation for Power System Dynamics with Variable and Low Inertia due to
Renewable Energy

by

Patricia Hidalgo-Gonzalez

A thesis submitted in partial satisfaction of the

requirements for the degree of

Master of Science

in

Electrical Engineering and Computer Sciences

in the

Graduate Division

of the

University of California, Berkeley

Committee in charge:

Professor Claire J. Tomlin, Chair
Professor Duncan S. Callaway

Fall 2019

Frequency Regulation for Power System Dynamics with Variable and Low Inertia due to
Renewable Energy

Frequency Regulation for Power System Dynamics with Variable and Low Inertia due to Renewable Energy

by Patricia Hidalgo-Gonzalez

Research Project

Submitted to the Department of Electrical Engineering and Computer Sciences, University of California at Berkeley, in partial satisfaction of the requirements for the degree of Master of Science, Plan II.

Approval for the Report and Comprehensive Examination:

Committee:
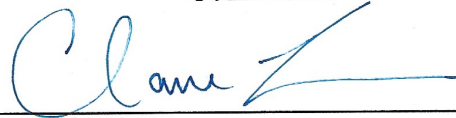
Professor Claire J. Tomlin
Research Advisor

12 / 05 / 2019

Date

Professor Duncan S. Callaway
Second Reader

12 / 5 / 2019

Date

When you work you are a flute through whose heart the whispering of the hours turns to music.

Kahlil Gibran, The Prophet, 1923.

Abstract

Frequency Regulation for Power System Dynamics with Variable and Low Inertia due to
Renewable Energy

by

Patricia Hidalgo-Gonzalez

Master of Science in Electrical Engineering and Computer Sciences

University of California, Berkeley

Professor Claire J. Tomlin, Chair

As more non-synchronous renewable energy sources participate in power systems, the sys-
tem's inertia decreases and becomes time dependent, challenging the ability of existing
control schemes to maintain frequency stability. System operators, research laboratories,
and academic institutes have expressed the importance to adapt to this new power system
paradigm. However, power dynamics have been modeled as time-invariant, by not modeling
the variability in the system's inertia. To address this, this work proposes a new modeling
framework for power system dynamics to simulate a time-varying evolution of rotational
inertia coefficients in a network. Power dynamics are modeled as a hybrid system with dis-
crete modes representing different rotational inertia regimes of the network. Using this new
modeling framework for power dynamics we study a framework to design a fixed learned
controller based on datasets of optimal time-varying LQR controllers. We test the perfor-
mance of the controller in a twelve-bus system. By adding virtual inertia we can guarantee
stability of high-renewable (low-inertia) modes. The novelty of our work is to propose a
design framework for a stable controller with fixed gains for time-varying power dynamics.
This is relevant because it would be simpler to implement a proportional controller with
fixed gains compared to a time-varying control.

Contents

List of Figures

List of Tables

Acknowledgments

I would like to thank my advisor Claire J. Tomlin for her unconditional support and trust. Claire, I profoundly enjoyed working with you. Your advice and critical thinking always allowed me to develop sound research questions and tackle them with the best suited tools from Control Theory and Machine Learning. Thanks to you, not only did I deepen my technical expertise, but I was also able to learn how to navigate life with compassion and assertiveness, an art in itself. I will treasure this lesson forever and will do my best to continue fostering it.

I would also like to thank my unofficial but unconditional advisor Duncan S. Callaway. Thanks, Duncan, for all the engaging conversations about power systems. You always made sure to keep me on my toes. This enabled me to work on a solid line of research to integrate renewable energy into our grids. I also admire how humble you are, and I hope to develop that quality through my career.

This section could not end without thanking my partner in crime, Rodrigo Henriquez-Auba. Thank you, Rodrigo, for all the fun times working together and attending conferences. All this work was also possible thanks to you. I look forward to continuing our collaborations in the years to come. Roel Dobbe, thank you for helping me to transition into this research space. I treasure our research discussions –developing ideas with you was incredibly intellectually engaging and entertaining. I look forward to continuing to work with you through our careers.

I would also like to thank my mom for her unconditional support and love. Alex Keller, thank you, too, for your love and support, specially through hard times. I am so fortunate to have you in my life. Anna Matsokina, I will be forever grateful for the spiritual growth I have been able to attain thanks to our friendship. I look forward to continue growing. And last but not least, I would like to thank Laurel Selvig. Thank you for joining the ride in the last part of my stay in graduate school. Your support and love has meant the world to me and I am excited to see what comes next.

Chapter 1

Introduction

1.1 Background and Motivation

In power systems, frequency will deviate from its nominal value when there is a mismatch between electricity generation and consumption [10]. There exists a set of mechanisms to prevent frequency excursions. The first automatic response when frequency starts to deviate is the inertial response. This inertial response is originated from the kinetic energy supplied to the grid by the synchronous generators. This inertia (present in rotating masses of generators and turbines) determines the instantaneous frequency change when imbalances of active power occur. Therefore, more inertia in the system will translate into a slower rate of change of the frequency. As the frequency starts deviating, some generators will respond automatically through governor response [4]. Governor response or droop control is an automatic control proportional to the frequency deviation. After droop control starts actuating, slower mechanisms (e.g. spinning reserves) participate to restore frequency to its nominal value [4].

It is a crucial aspect for the operation and stability of electrical systems to maintain the grid frequency within acceptable ranges. Nowadays, large shares of renewable energy sources (RES) are being integrated into power systems. Several countries have set ambitious goals for the future to provide more electricity using renewable energy [13] and/or reducing their CO_2 emissions. This global drive will steer the power system to a grid dominated by RES [18]. In this scenario, renewable sources, such as wind and solar, are usually connected to the grid through inverters, which decouple their rotational inertia (if existing) from the grid.

Usually, depending on the configuration of the inverters, no inertial response is delivered to the grid. With this increasing penetration of RES, the global system inertia of the power systems is decreasing and time-varying. This can provoke an increment in the variation of frequency under abrupt changes in generation and demand. If no actions are taken, this can lead to cases in which standard frequency control schemes are too slow to mitigate arising contingencies [16].

A possible solution for this issue is to use RES inverters or large scale storage to provide

inertia. This can be done by operating the RES or storage's inverters as virtual inertia (control proportional to the derivative of the frequency), that could allow large penetration of RES without jeopardizing the system's stability [1]. Previous work studying virtual inertia can be found in the literature. In [15], a detailed survey of different virtual inertia techniques, topologies and future directions are presented. [19] introduces the concept of inverters that emulate the response of a synchronous machine. [12] proposes a new controller to address low inertia. This work argues that virtual inertia could amplify noise in an unbounded manner. The work from [17] discusses virtual inertia (or inertia mimicking) by enabling inverter-connected generation units to quickly modify their power output via Model Predictive Control (MPC), mimicking the dynamic response of conventional units. In a similar line of work, [3] studies the effect that changes in inertia have on power system stability, and how to best place devices providing virtual inertia. Most recently [14] studied optimal placement of virtual inertia in different nodes of a network.

1.2 Research Gap and Outline

The work presented in this thesis is motivated by the need to better represent power system dynamics in the presence of RES connected to the grid by inverters. To address this need, Chapter 2 introduces a new framework to model frequency dynamics as a time-varying system due to the variability of the inertia coefficients in a network. More specifically, we propose to model power dynamics in a network as a Switched Affine Hybrid system where the time-varying components are the inertia coefficients of the nodes in a grid.

The natural question that stems from facing new frequency dynamics due to the presence of RES is how to design a controller that is easy to implement in power systems and that has stability guarantees. Chapter 3 addresses this question by presenting a framework to learn a fixed and stable frequency controller that is able to return the frequency to its nominal value for any mode of the hybrid system.

This work has been published at the IEEE Conference on Decision and Control and the IEEE Power & Energy Society General Meeting.

Chapter 2

Power System Dynamics as a Hybrid System

2.1   Introduction

The work discussed in this chapter corresponds to the publication titled "Frequency Regulation in Hybrid Power Dynamics with Variable and Low Inertia due to Renewable Energy" by Patricia Hidalgo-Gonzalez, Roel Dobbe, Rodrigo Henriquez-Auba, Duncan S. Callaway and Claire J. Tomlin [8]. We presented this publication at the 57th IEEE Conference on Decision and Control in Miami, Florida, United States.

   The body of work around virtual inertia has mostly focused on the effects on the grid and on its optimal allocation. The frequency dynamics have been modeled as a time-invariant system. However, when we take into account the nature of the changes of rotational inertia in the grid, it requires a new modeling framework that represents this time dependence and variability of the system's inertia. Thus, the contributions of this work are the following:

- We propose a new modeling framework for power system dynamics to simulate a time-varying evolution of rotational inertia coefficients in the network. To do this, we model power dynamics as a hybrid system [2] where each mode corresponds to a rotational inertia regime. At each time step of the simulation the dynamical system mode can switch to a different rotational inertia mode in an exogenous fashion.

- We test the performance of two classical controllers from the literature (optimal closed-loop controller from MPC and virtual inertia placement) in this new hybrid modeling framework.

- We propose a new controller (Dynamic Inertia Placement) to more efficiently address low and variable inertia in the grid.

   We conclude that the new modeling framework we develop is necessary to design controllers that address frequency regulation in power systems with high RES penetration. We

also find that the optimal linear closed-loop controller (referred as Linear MPC in this work) performs best in terms of cost and energy injected/absorbed to control frequency. Lastly, we find that our proposed controller for Dynamic Inertia Placement (when modeling dynamics with variable inertia) is more efficient in terms of cost and energy usage than the classical Inertia Placement from the literature.

The rest of the chapter is organized as follows: Section 2.2 presents the problem formulation, Section 2.3 shows simulations from a study case, and finally Section 2.4 concludes with our main findings.

2.2 Problem Formulation

Power system dynamics as a hybrid system

We consider an electric power network modeled as a graph with N nodes and $N(N-1)/2$ possible edges connecting them. The swing equation model used for this network is based on [10], where dynamics are given by

$$m_i \ddot{\theta}_i + d_i \dot{\theta}_i = p_{\text{in},i} - \sum_j b_{ij}(\theta_i - \theta_j), \quad i \in \{1, ..., N\} \tag{2.1}$$

m_i corresponds to the equivalent rotational inertia in node i, d_i is the droop control, $p_{\text{in},i}$ represents the power input at node i, b_{ij} is the susceptance of the transmission line between nodes i and j, and θ_i is the voltage phase angle at node i. The state space representation of the model is given by

$$\begin{bmatrix} \dot{\theta} \\ \dot{\omega} \end{bmatrix} = \begin{bmatrix} 0 & I \\ -M^{-1}L & -M^{-1}D \end{bmatrix} \begin{bmatrix} \theta \\ \omega \end{bmatrix} + \begin{bmatrix} 0 \\ M^{-1} \end{bmatrix} p_{\text{in}} \tag{2.2}$$

where the states correspond to the stacked vector of angles and frequencies at each node $(\theta, \omega) \in \mathbb{R}^{2n}$, $M = \text{diag}(m_i)$ is a diagonal matrix with rotational inertia coefficients, $D = \text{diag}(d_i)$ is a diagonal matrix with droop control coefficients, p_{in} corresponds to the power input, and $L \in \mathbb{R}^{n,n}$ is the Laplacian of the network. The network Laplacian is defined as $\ell_{ij} = -b_{ij}$ when $i \neq j$, and $\ell_{ii} = \sum_{i \neq j} b_{ij} + y_{i,s}$, where $y_{i,s}$ are all shunt admittances connected at node i.

In the traditional paradigm of power systems, where generation has been dominated by thermal generation, the inertia at each node m_i has been considered constant. However, in recent years, it has been observed that due to the increase in generation from RES, the rotational inertia in the network has become lower and time-varying [16], [5]. In order to model power dynamics taking into account the variability of inertia at each node, our work proposes a new framework for modeling frequency dynamics. Instead of assuming equation (2.2) as a time-invariant dynamical system, we propose to model it as a Switched Affine hybrid system [2], where each mode will be given by a predetermined set of values of m_i at each node. The switching between the different m modes depends on the current online

generators. In this work, the mix of online generators at each time step t is modeled as an exogenous input. Therefore, power dynamics will be given by

$$\begin{bmatrix} \dot{\theta} \\ \dot{\omega} \end{bmatrix} = \begin{bmatrix} 0 & I \\ -M_q^{-1}L & -M_q^{-1}D \end{bmatrix} \begin{bmatrix} \theta \\ \omega \end{bmatrix} + \begin{bmatrix} 0 \\ M_q^{-1} \end{bmatrix} p_{\text{in}} \tag{2.3}$$

where M_q represents the inertia matrix M in the current mode $q \in \{1, ..., m\}$. The switching between modes can occur from any time step t to $t + 1$, and it is given by a uniform distribution with the following possible outcomes:

- No change of inertia

- Increase of inertia

- Decrease of inertia

Thus, the evolution over time of the matrix M_q is modeled as a Markov Chain. For simplicity, for a given mode q we assume the same inertia coefficients for all nodes. Section 2.3, describes in more detail the assumption on inertia coefficients at the nodes of the network.

Power input at node i, can be expressed as

$$p_{in} = (\delta + u), \quad \delta_i \sim N(0, 0.1) \quad i = 1...N \tag{2.4}$$

where δ is a time-varying vector whose components, δ_i, are disturbances at each node i (modeled as white noise), and the vector u is the controller (power injection). Thus, equation (2.3) can be written as

$$\begin{bmatrix} \dot{\theta} \\ \dot{\omega} \end{bmatrix} = \begin{bmatrix} 0 & I \\ -M_q^{-1}L & -M_q^{-1}D \end{bmatrix} \begin{bmatrix} \theta \\ \omega \end{bmatrix} + \begin{bmatrix} 0 \\ M_q^{-1} \end{bmatrix} (\delta + u) \tag{2.5}$$

$$\begin{bmatrix} \dot{\theta} \\ \dot{\omega} \end{bmatrix} := A_q \begin{bmatrix} \theta \\ \omega \end{bmatrix} + B_q (\delta + u) \tag{2.6}$$

In this hybrid formulation, the design of the optimal controller u is more complex than in the traditional linear time-invariant (LTI) case. Recent work has shown the relevance of the optimal placement of virtual inertia in the grid [14], which expanded on previous work that studied the effects of rotational inertia in a network [3]. In this study we build on this work by including the evolution over time of the rotational inertia at each node. Using receding horizon Model Predictive Control we study three different designs for the controller u in equation (2.5).

Optimal frequency control for low and time-varying rotational inertia coefficients

In order to minimize an objective function with the states and controller as variables, we consider three possible controllers u. In addition, we take into account a constraint to maintain the frequency ω at all time t in a predefined safe interval. The receding horizon MPC formulation can be summarized by the following optimization problem:

$$\min_{x(t),u(t)} \quad \int_{t=t_0}^{T} x(t)^{\top}Qx(t) + u(t)^{\top}Ru(t)dt \tag{2.7}$$

$$\text{s.t. } x(t_0) = x_0 \tag{2.8}$$

$$\dot{x}(t) = A_q x(t) + B_q\big(\delta(t) + u(t)\big), \quad t \in (t_0, T) \tag{2.9}$$

$$\underline{b} \leq x(t) \leq \bar{b}, \quad t \in (t_0, T) \tag{2.10}$$

$$\delta_i(t) \sim N(0, 0.1), \quad i \in \{1, ..., N\}, \quad t \in (t_0, T) \tag{2.11}$$

where x is the vector of the states (θ, ω), u the controller, Q and R are symmetric positive definite matrices, t_0 the initial time, T the final time, $\underline{b}$ and $\bar{b}$, lower and upper bounds for the frequency, and x_0 the initial state. As it was mentioned earlier, the hybrid modes q transition at each time step t using a Markov Chain. We consider three designs for optimal controllers u obtained using receding horizon MPC:

1. Linear MPC:

$$u_i(t) \text{ unconstrained}, \quad i \in \{1, ..., N\}, \quad t \in (t_0, T) \tag{2.12}$$

2. Inertia Placement [14]:

$$u_i(t) = -M_i\dot{\omega}_i, \quad i \in \{1, ..., N\}, \quad t \in (t_0, T) \tag{2.13}$$

3. Dynamic Inertia Placement:

$$u_i(t) = -M_i(t)\dot{\omega}_i, \quad i \in \{1, ..., N\}, \quad t \in (t_0, T) \tag{2.14}$$

The receding horizon MPC formulation (2.7) - (2.12) is classified as a quadratic problem with linear constraints, thus a convex problem. The receding horizon MPC formulation for inertia placement, (2.7) - (2.11), (2.13) and (2.7) - (2.11), (2.14), are non convex problems. To model the first formulation we use CVX [6], [7]. To model the non convex formulations we use the parser YALMIP [11], and solved the optimization problem using an interior point method.

In the case of the Linear MPC formulation, the controller $u_i(t)$ does not have any constraints imposed. Implying that the feasible set of the Linear MPC formulation and the

feasible set of the problem given by (2.7) - (2.11) are equivalent. The Dynamic Inertia Placement formulation introduces a new variable $M_i(t)$. This new variable needs to be optimized for all nodes i at all time steps t. The controller $u_i(t)$ is constrained to be equal to $-M_i(t)\dot{\omega}_i$, serving as virtual inertia. The fact that the Dynamic Inertia Placement formulation has an extra set of constraints on $u_i(t)$ implies that the feasible set of this problem is contained in the feasible set of the Linear MPC formulation. Finally, the Inertia Placement formulation, in addition to having the constraint on the structure of $u_i(t)$ as the Dynamic Inertia Placement had, it has an additional set of constraints. This extra set of constraints forces $M_i(t)$ to be equal to M_i for all t. In other words, the design of the virtual inertia controller cannot be specific to a node and time, but a fixed design over time for each node. Thus, the Inertia Placement formulation has its feasible set contained in the feasible set of the Dynamic Inertia Placement formulation. In summary, the Linear MPC formulation has the largest feasible set, followed by the Dynamic Inertia Placement which has more constraints. Finally the Inertia Placement formulation comes in third place with the most restrictive feasible set. Due to this, we expect solutions u^* from the Linear MPC formulation to be best, attaining the lowest value in its objective function. We expect the Dynamic Inertia Placement case to come in second place with a higher optimal value for its objective function compared to the Linear MPC formulation. The formulation with the highest optimal value of its objective function would be the Inertia Placement formulation.

One of the contributions of this work is to assess the grid's performance when virtual inertia is optimized over time and location (Dynamic Inertia Placement). We also compare inertia placement with the Linear MPC formulation. The latter sheds light on how the performance of frequency dynamics could improve with a more flexible controller (not constrained to be a derivative control law as inertia placement is).

In Section 2.3 we compare these three formulations. We utilize the study case (originally from [10]) used in some recent virtual inertia placement work [3] and [14].

2.3 Case Study: Twelve-Bus Three-Region Network

Data description

The twelve-bus three-region network used in this study has also been used in [10], [3], and [14]. The full network was modeled, without using any simplifications (e.g. no Kron reduction of the graph). Therefore, twelve nodes were modeled with two states each (angle and frequency). Table 2.1 shows the parameters of the network.

The positive definite matrices Q and R from the objective function in problem (2.7) that we use in the case study are the identities. With this selection we are equally penalizing frequency deviations from zero and energy injection/absorption from the controller. This assumption can be changed to, for example, represent the real economic cost to the grid that frequency deviations and energy injection/absorption from the controller represent. This in itself is an open research question.

Table 2.1: Parameters for the twelve-bus three-region case study [10], [3].

Parameter	Value
Transformer reactance	0.15 p.u.
Line impedance	(0.0001 + 0.001j) p.u./km
Base voltage	230 kV
Base power	100 MVA
Droop control	1.5 %/%
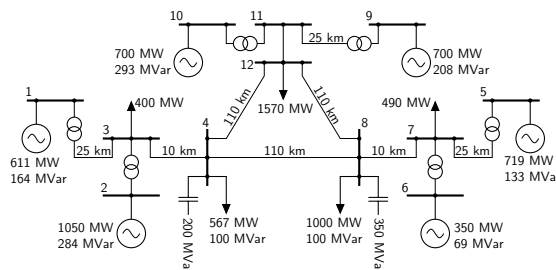
Figure 2.1: Case study: Twelve-bus three-region network from [10], [14], and [3].

As it was discussed in Section 2.2, the inertia matrix M is modeled as a diagonal matrix $\text{diag}(m_i)$, whose elements m_i correspond to the rotational inertia at the bus i. We assume the same rotational inertia in all buses for a given time step t ($m_i(t) = m(t)$ for all i). This implies a similar fraction of renewable energy generation for all nodes, which is common in large networks. However, this assumption can be easily extended. In this work, we model the variability of the rotational inertia in the system as a hybrid system switching modes as the inertia changes. Each mode of the hybrid system is given by one value of inertia. For the study case we predefined possible inertia values for the system: $\{0.1, 0.5, 1, 1.5, 2, 2.5, 3, 3.5, 5, 9\}$. The average of this set of possible inertia values is 2.8 seconds, which is equivalent to having 28 percent of thermal generation (10 s of inertia) and 72 percent of RES with zero inertia. Each simulation starts with 2 seconds of inertia, and from there- based on a uniform distribution draw- the inertia (hybrid mode) of the system at time $t+1$ will remain the same, increase, or decrease (Markov Chain with 1/3 probability for each possible mode transition). This process is repeated until each time step t in the time horizon T has assigned a rotational inertia mode.

The safety bounds for frequency are ± 0.1 Hz ($\underline{b}$ and $\bar{b}$ in equation (2.10)).

Results

Each receding horizon MPC formulation is run for eight time steps (T) and 100 possible realizations (or scenarios) from the Markov Chain of the rotational inertia matrix M_q. Thus,

Table 2.2: Summary: mean and standard deviation of objective function J^*, optimal control u^*, and frequency ω.

Moments	Linear MPC	Inertia Placement	Dynamic Inertia Placement
$\mu(J^*)$	0.17	0.92	0.24
$\sigma(J^*)$	0.07	1.66	0.30
$\mu(u^*)$ p.u.	-0.004	-0.018	-0.005
$\sigma(u^*)$ p.u.	0.13	0.29	0.15
$\mu(\omega)$ mHz	-0.34	0.93	8.10
$\sigma(\omega)$ Hz	0.07	0.04	0.05

for each formulation we obtain an optimal value of the objective function at each time step and each scenario (i.e. 800 values). The number of nodes, N, is 11 because node 11 and 12 are the same (refer to Fig. 2.1). We also obtain N control actions (one per node) for each time step and for each scenario (i.e. 8800 values), and N frequency measurements for each time step and for each scenario (i.e. 8800 values). Using these sets of results we calculate moments and show histograms for the three formulations in order to compare them.

Table 2.2 shows the mean and standard deviation of the set of optimal values of the objective function (J^*) at all times t and all scenarios for the three formulations. The same moments are shown for optimal control (u^*) and frequency (ω) for the three optimization problems. As discussed in Section 2.2, the Linear MPC formulation shows the lowest average and standard deviation values in its objective function compared to the other two formulations. The average of the objective function for the Linear MPC is 0.17 cost units, and its standard deviation 0.07. In the case of the average, it corresponds to 18 percent of the average in the Inertia Placement formulation and 71 percent of the average in the Dynamic Inertia Placement case. This result can be interpreted as the Inertia Placement formulation resulting in non zero frequency deviations and non zero control actions 82 percent more of the time compared to the Linear MPC formulation (on average). This result sheds light on the suboptimality of the virtual (dynamic and static) inertia controllers compared to the closed-loop formulation (Linear MPC). Thus, there is an incentive to continue designing controllers that try to address low and variable inertia coefficients in the grid.

Another relevant result is the fact that our proposed Dynamic Inertia Placement formulation provides better performance than the Inertia Placement formulation in terms of average cost and energy usage in the controller u^*. This is expected as well because we provide more flexibility for the controller to inject/absorb energy depending on not only the node, but also on the time step. The average objective value in the Dynamic Inertia Placement formulation is 39 percent of the average optimal value of the objective function in the Inertia Placement case.

Fig. 2.2 and 2.3 show histograms of the optimal controllers u^* for the Inertia Placement
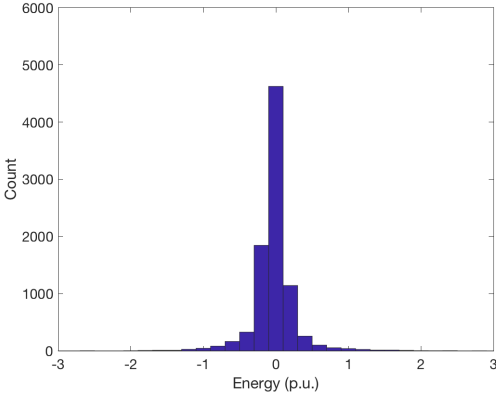
Figure 2.2: Inertia Placement: Histogram of optimal controller u^* at all nodes, all time steps, and all scenarios.
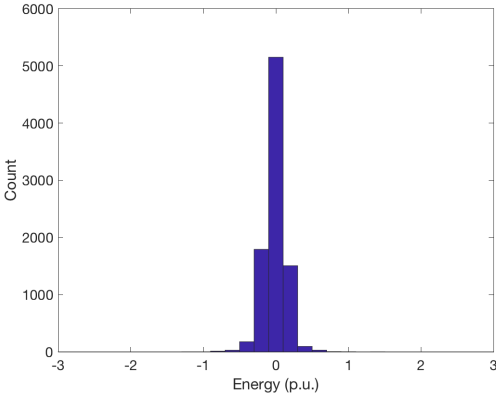
Figure 2.3: Dynamic Inertia Placement: Histogram of optimal controller u^* at all nodes, all time steps, and all scenarios.

formulations. Statistics in Table 2.2 show that the optimal controller for the Linear MPC formulation case uses less energy on average to maintain the frequency within the allowed bounds. Its maximum injection/absorption is between ± 0.3 p.u. (not shown in Table 2.2). The optimal injection from the Inertia Placement formulation ranges between -2.6 and 2.8 p.u. to maintain the same safety bounds for the frequency. The control range from the Dynamic Inertia Placement is smaller (-1.2 and 1.4 p.u.) compared to the spread observed in the energy absorbed/injected by the Inertia Placement controller. Therefore, it shows a more efficient frequency control design.
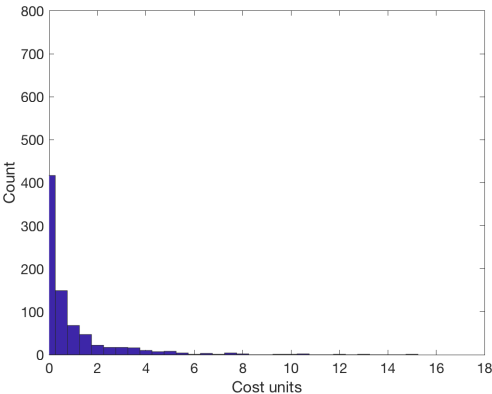
Figure 2.4: Inertia Placement: Histogram of optimal cost J^* at all time steps and all scenarios.
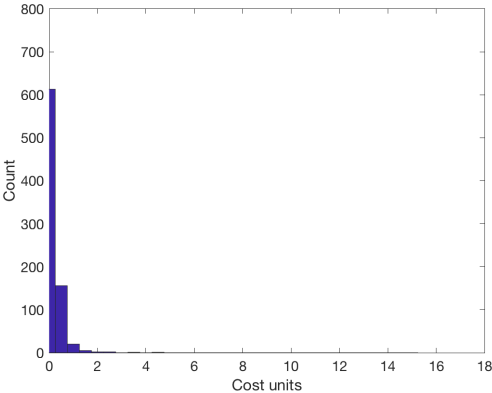
Figure 2.5: Dynamic Inertia Placement: Histogram of optimal cost J^* at all time steps and all scenarios.

Fig. 2.4 and 2.5 show histograms of optimal costs for the Inertia Placement formulations. The moments in Table 2.2 show that the optimal values for the Linear MPC formulation are concentrated around zero. However, the Inertia Placement formulations show more spread, reaching extreme costs of 15 units (Inertia Placement) and 4.3 units (Dynamic Inertia Placement). The distribution of the costs for the Dynamic Inertia Placement controller is more skewed and its tail does not reach as high of values (Fig. 2.5) compared to the tale of the cost distribution in the Inertia Placement design (Fig. 2.4).

2.4 Conclusions

We propose a new modeling framework for power systems dynamics that captures the variability of rotational inertia over time. Our proposed model is a Switched Affine hybrid system, whose modes change based on the change of inertia in the nodes. The transition from one mode to another is determined by a Markov Chain at each time step of the simulation. With this new framework, we test two standard frequency control designs and propose a third design: Linear MPC, Inertia Placement, and Dynamic Inertia Placement. As expected, the Linear MPC formulation is better in terms of cost and energy injection/absorption to control frequency. This finding encourages researchers to continue designing controllers in order to attain such optimality without having to optimize in real time (closed-loop MPC).

Another relevant finding is the fact that the Dynamic Inertia Placement proves to be more efficient in terms of cost and energy usage of the controller compared to the classical Inertia Placement case. This finding sheds light on the importance of modeling dynamics over time assuming temporal variability in the system's inertia. Additionally, it highlights the importance of designing a more flexible controller that would adapt over time. For future work we plan to study stability of the hybrid system and design a controller that is more efficient in terms of energy usage than the current virtual inertia schemes. We also plan to characterize the disturbances at each node of the network and to model the switching of modes of the hybrid system with data-driven approaches.

Chapter 3

Frequency Regulation using Data-Driven Control

3.1 Introduction

The work in this chapter corresponds to the publication titled "Frequency Regulation using Data-Driven Controllers in Power Grids with Variable Inertia due to Renewable Energy" by Patricia Hidalgo-Gonzalez, Rodrigo Henriquez-Auba, Duncan S. Callaway and Claire J. Tomlin [9]. We presented this work at the 2019 IEEE Power & Energy Society General Meeting in Atlanta, Georgia, United States.

Our earlier work [8], introduces a new modeling framework for power system dynamics to simulate a time-varying evolution of rotational inertia coefficients in the network. To do this, power dynamics are modeled as a hybrid system in which each mode corresponds to a rotational inertia regime. The novelty of this work is the design of a fixed and stable frequency controller under a paradigm of time-varying inertia. We choose a fixed controller because it is simpler to implement (compared to a time dependent controller) given the existing droop control in the grid. In addition, the controller we propose does not require information about the current hybrid mode of the system or its uncertainty. Thus, our contributions are the following:

- In the time-varying framework for power dynamics, we design a controller with fixed gains, proportional to the system's states (angles and frequencies). We design the controller by learning its parameters from the optimal control solution of a hybrid systems linear-quadratic regulator (LQR) formulation of power dynamics.

- For each mode of the hybrid system, we test the performance of the learned controller against the optimal time-varying controller from the LQR formulation.

- We add virtual inertia control (linear on the derivative of the frequency) to guarantee stability for all modes of the hybrid system when using the learned controller.

We conclude that for the hybrid power dynamics formulation it is possible to design, through learning, a static frequency controller proportional to the system's states that performs similarly to the optimal time-varying controller from LQR. It is possible to guarantee stability for the hybrid system when we add virtual inertia to the learned control.

The rest of the chapter is organized as follows: Section 3.2 presents the problem formulation, Section 3.3 analyses stability of the hybrid system and shows the performance of the controller in different settings, and finally Section 3.4 concludes with our main findings.

3.2   Problem Formulation

Power grid dynamics as a hybrid system

We consider an electric power grid modeled as a graph with n nodes and $n(n-1)/2$ possible edges connecting them. The swing equation model, based on the direct current approximation [14], used for the network is given by

$$m_i\ddot{\theta}_i + d_i\dot{\theta}_i = p_{\text{in},i} - \sum_{j\in\mathcal{N}_i} b_{ij}(\theta_i - \theta_j), \quad i \in \{1, \ldots, N\} \tag{3.1}$$

where m_i corresponds to the equivalent rotational inertia in node i, d_i is the droop control, $p_{\text{in},i}$ represents power mismatch at node i, $\mathcal{N}_i$ is set of nodes connected by an edge to node i, b_{ij} is the susceptance of the transmission line between nodes i and j, and θ_i is the voltage phase angle at node i. The state space representation of the model can be written as

$$\begin{bmatrix} \dot{\theta} \\ \dot{\omega} \end{bmatrix} = \begin{bmatrix} 0 & I \\ -M^{-1}L & -M^{-1}D \end{bmatrix} \begin{bmatrix} \theta \\ \omega \end{bmatrix} + \begin{bmatrix} 0 \\ M^{-1} \end{bmatrix} p_{\text{in}} \tag{3.2}$$

where the states correspond to the stacked vector of angles and frequencies at each node $(\theta^\top, \omega^\top)^\top \in \mathbb{R}^{2n}$, $M = \text{diag}(m_i)$ is a diagonal matrix with rotational inertia coefficients, $D = \text{diag}(d_i)$ is a diagonal matrix with droop control coefficients, I is the $n \times n$ identity matrix, p_{in} corresponds to the power input, and $L \in \mathbb{R}^{n,n}$ is the Laplacian of the network. The network Laplacian is defined as $\ell_{ij} = -b_{ij}$ when $i \neq j$, and $\ell_{ii} = \sum_{j\in\mathcal{N}_i} b_{ij}$.

Thermal generators are predominant in the traditional paradigm of power systems. In this setting, the equivalent inertia can be considered as constant over time. However, due to the increasing penetration of RES, the equivalent rotational inertia has become lower and time-varying [16, 5]. This work uses the modeling framework first introduced in [8] to represent the time dependence in inertia at each node. Frequency dynamics are modeled as a Switched-Affine hybrid system [2], where each mode has a predetermined set of values of equivalent inertia m_i at each node [8]. The evolution of the inertia on the system depends on the current online generators and the connected power electronics converter. In this work, the inertia at each time step t evolves as an exogenous input over different modes. Thus,

the power dynamics are given by

$$\begin{bmatrix} \dot{\theta} \\ \dot{\omega} \end{bmatrix} = \underbrace{\begin{bmatrix} 0 & I \\ -M_{q(t)}^{-1}L & -M_{q(t)}^{-1}D \end{bmatrix}}_{\hat{A}_{q(t)}} \begin{bmatrix} \theta \\ \omega \end{bmatrix} + \underbrace{\begin{bmatrix} 0 \\ M_{q(t)}^{-1} \end{bmatrix}}_{\hat{B}_{q(t)}} p_{\text{in}} \tag{3.3}$$

where $M_{q(t)}$ represents the inertia matrix in the mode $q(t) \in \{1, \ldots, m\}$. Using a zero-order hold discretization with time step T_s, we obtain the discretized time-varying dynamics

$$x_{t+1} = A_{q(t)}x_t + B_{q(t)}u_t \tag{3.4}$$

where x_t is the stacked vector of discretized angles and frequencies, $(\theta_t^\top, \omega_t^\top)^\top$, u_t is the control action by generators and converters, $A_{q(t)} = \exp(\hat{A}_{q(t)}T_s)$ and $B_{q(t)} = \int_0^{T_s} \exp(\hat{A}_{q(t)}\tau)\hat{B}_{q(t)}d\tau$
.

In this work, the switching between modes occurs between each time step, and it is given by a uniform distribution with the following possible outcomes: no change of inertia, increase of inertia, or decrease of inertia. For simplicity, for a given mode q we assume the same inertia coefficient for all nodes $M_q = m_q I_{n \times n}$. Using an LQR formulation we study the problem of returning to a steady-state configuration x_{ss}, assuming a perturbed initial condition $x_0 \neq x_{\text{ss}}$ due to a contingency.

Optimal frequency control for low and time-varying rotational inertia coefficients

To minimize an objective function where the states and controllers are decision variables we consider the LQR formulation

$$\begin{aligned} \min_{\boldsymbol{x}, \boldsymbol{u}} \quad & \sum_{t=0}^{T} x_t^\top Q x_t + u_t^\top R u_t \\ \text{s.t.} \quad & x_0 = x^{(0)} \\ & x_{t+1} = A_{q(t)}x_t + B_{q(t)}u_t, \ t \in \{0, T-1\} \end{aligned} \tag{3.5}$$

where Q is a positive semidefinite matrix, R is a positive definite matrix, and $x^{(0)}$ is the initial state. Depending on the modeling goal, matrices Q and R can be modified to promote a specific behavior. The optimal solution of (3.5) for a fixed mode q in the entire time horizon (i.e. a linear time-invariant system) and with $T \to \infty$, can be found via the discrete time algebraic Ricatti equation [2]:

$$\begin{aligned} P_q &= A_q^\top P_q A_q - A_q^\top P_q B_q (R + B_q^\top P_q B_q)^{-1} B^\top P_q A_q + Q \\ K_q &= (R + B_q^\top P_q B_q)^{-1} B_q^\top P_q A_q \\ u_t &= -K_q x_t \end{aligned} \tag{3.6}$$

For a hybrid system with time-varying inertia, (3.5) is a Quadratic Programming problem that can be solved directly, using for example CVX [6]. We use the solution of (3.5) as a benchmark of an optimal controller for our problem.

Data-driven based controller

In the presented framework of variable inertia we are interested in learning a time-invariant controller of the form $u_t = -K_{\mathrm{L}}x_t$ where K_{L} is a constant matrix. The training dataset $(\boldsymbol{x}^{(k)}, \boldsymbol{u}^{(k)})$ we use comes from the optimal solution to (3.5) under different scenarios $k = \{1, \ldots, K\}$. The learning algorithm we use is least-squares:

$$\min_{K_{\mathrm{L}}} \ \sum_{k=1}^{K} \sum_{t=1}^{T} \left\| u_t^{(k)} - K_{\mathrm{L}}x_t^{(k)} \right\|_2^2 \tag{3.7}$$

It is interesting to notice that when we solve (3.5) for a single mode q (in the entire time horizon) and a sufficiently long time horizon T, least-squares returns the analytical solution K_q from the LQR problem (3.6). This is because the optimal controller from (3.5) is linear on the states, and with sufficient training data $(\boldsymbol{x}^{(k)}, \boldsymbol{u}^{(k)})$, (3.7) is a convex optimization program that achieves K_q, and hence the optimal value is equal to zero.

We assume a stressed case in which the equivalent inertia can change rapidly over time. Thus, inertia is allowed to change over time steps in each scenario. However, an equivalent training set can be generated by fixing the mode q at each scenario k, and only changing the mode between different scenarios. Each scenario in this training set would represent, for instance, a different hour of the year. During an hour, inertia could be considered fixed, and a different optimal controller would be obtained for each scenario.

Incorporating virtual inertia in the system

Depending on how we generate the training set $(\boldsymbol{x}^{(k)}, \boldsymbol{u}^{(k)})$, the controller we propose may not be stable in modes where the inertia is too low. The learned controller may not be fast enough to compensate the rate of change of the frequency. As an alternative, a controller that depends on the derivative of the frequency, $K_{\mathrm{V}}\dot{\omega}$, can be used as a virtual inertia resource for the system. Indeed, consider the fixed inertia continuous time system and assume a controller of the form

$$u = -K_{\mathrm{L}}(\theta^{\top}, \omega^{\top})^{\top} - K_{\mathrm{V}}\dot{\omega} = -K_{\mathrm{L}}x - \tilde{K}_{\mathrm{V}}\dot{x} \tag{3.8}$$

where $\tilde{K}_{\mathrm{V}} = [0 \ \ K_{\mathrm{V}}]$, then:

$$\dot{x} = \begin{bmatrix} 0 & I \\ -M^{-1}L & -M^{-1}D \end{bmatrix} x - \begin{bmatrix} 0 \\ M^{-1} \end{bmatrix} (K_{\mathrm{L}}x + \tilde{K}_{\mathrm{V}}\dot{x})$$

Table 3.1: Parameters for the twelve-bus three-region case study [3], [8] and [10].

Parameter	Value
Transformer reactance	0.15 p.u.
Line impedance	(0.0001 + 0.001j) p.u./km
Base voltage	230 kV
Base power	100 MVA
Droop control	1.5 %/%

Rearranging terms the system can be written

$$\dot{x} = (I + \hat{B}\tilde{K}_V)^{-1}(\hat{A} - \hat{B}K_{\mathrm{L}})x$$
$$= \begin{bmatrix} 0 & I \\ -\tilde{M}^{-1}(L + K_{\mathrm{L},\theta}) & -\tilde{M}^{-1}(D + K_{\mathrm{L},\omega}) \end{bmatrix} x$$

where $\tilde{M} = M(I + M^{-1}K_V) = M + K_V$ provides a new system wide equivalent inertia due to the virtual inertia controller K_V. To determine a proper K_V we develop a heuristic using a bisection method. We assume K_V of the form $K_V = k_v I_{n \times n}$. Iterating over k_v, and assuming that $\dot{x}$ in the right hand side of the discretized system can be approximated by $[x_t - x_{t-1}]T_s^{-1}$, we modify k_v until the discretized closed loop system for the low inertia modes has all its eigenvalues inside the unit circle, making it stable.

3.3 Simulations and Results

Data description

Using MATLAB® we modeled a twelve-bus three-region network that has also been used in [3], [14], [8] and [10]. Each node has two states (angle and frequency). Table 3.1 shows the parameters of the network.
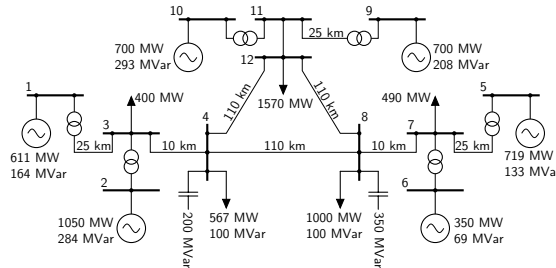
Figure 3.1: Case study: Twelve-bus three-region network from [3], [14], [8] and [10].

We assume the same rotational inertia in all buses for a given time step t ($m_i(t) = m(t)$ for all i). This implies a similar fraction of renewable energy generation for all nodes, but this assumption can be easily extended. Each mode of the hybrid system is given by one value of inertia. For the study case we predefined possible inertia values for the system: $m_q \in \{0.2, 0.5, 1, 1.5, 2, 2.5, 3, 3.5, 5, 9\}$. The average of this set of possible inertia values is 2.8 seconds, which is equivalent to having 28 percent of thermal generation (10 s of inertia) and 72 percent of RES with zero inertia. Each simulation starts with 2 seconds of inertia (mode q_5), and from there– based on a uniform distribution draw– the inertia (hybrid mode) of the system at time $t+1$ will remain the same, increase, or decrease. In our simulations we only allow the possibility to change modes every 1, 4 or 10 time steps. For all the simulations we use a time step of $T_s = 0.01$s. We generate $K = 400$ scenarios of 7 seconds each ($T = 700$). The initial conditions we use in (3.5) are randomly drawn from a normal distribution with zero mean and unitary variance. The training set we use to learn the controller K_L using (3.7) are the optimal solutions $(\boldsymbol{x}^{(k)}, \boldsymbol{u}^{(k)})$ from (3.5).

Stability analysis

The design of the controller K_L through learning provides a stable closed loop system $A_q - B_q K_L$ for every mode except for q_1. To correct this issue we use an approximated virtual inertia controller $\tilde{K}_V(x_t - x_{t-1})T_s^{-1}$ with $\tilde{K}_V = [0 \quad K_V]$. The new dynamics can be written as:

$$
\begin{aligned}
x_{t+1} &= A_q x_t + B_q[-K_L x + T_s^{-1}\tilde{K}_V(x_t - x_{t-1})] \\
&= [A_q - B_q(K_L - T_s^{-1}\tilde{K}_V)]x_t - T_s^{-1}B_q\tilde{K}_V x_{t-1}
\end{aligned}
$$

Augmenting the states as $z_{t+1} = (x_t^\top, x_{t+1}^\top)^\top$, our new system can be written as:

$$
z_{t+1} = \begin{bmatrix} 0_{2n\times 2n} & I_{2n\times 2n} \\ -T_s^{-1}B_q\tilde{K}_V & A_q - B_q(K_L - T_s^{-1}\tilde{K}_V) \end{bmatrix} z_t \tag{3.9}
$$

For the learned controller, adding a virtual controller of the form $K_V = 0.15 I_{n\times n}$ results in eigenvalues of the augmented system for mode q_1 inside the unitary circle. This is depicted in Figure 3.2, where it can be observed that there are two modes that are unstable for the closed loop system only using the learned controller (in red). When we incorporate the virtual inertia controller all modes are stable (in blue).

Controllers' comparison for fixed inertia

For each mode q, we compare the performance of the learned controller K_L and the learned controller with virtual inertia, $K_L +$ VI, against the optimal controller from the LQR formulation. Table 3.2 shows peaks (ℓ_∞ norm), ℓ_2 and ℓ_1 norms for frequency deviations f and control inputs u, and objective function values J for the different controllers under different inertia modes (columns). The values in table 3.2 represent increases in percentage
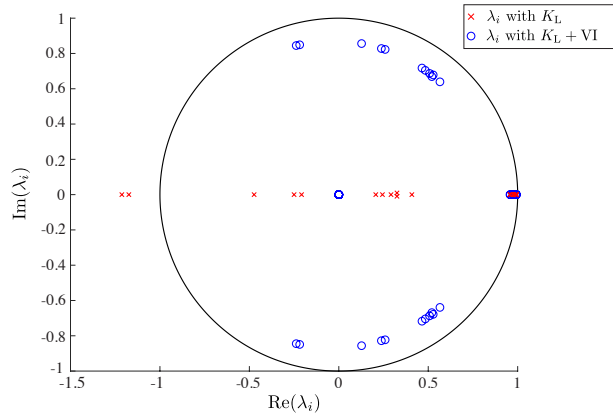
Figure 3.2: Eigenvalue placement for the closed loop system in mode q_1 using the learned controller K_{L} (crosses) and adding virtual inertia control $K_{\mathrm{L}} + \mathrm{VI}$ (circles).

with respect to the metrics for the LQR controller. The learned controller is unstable in the critical inertia regime (q_1, lowest inertia). When adding virtual inertia, the controller becomes stable. The objective values for the data-driven controllers are greater than for the LQR. This is intuitive because the learned controllers have fixed parameters over time while the LQR changes its parameters for each mode. The ℓ_2 norm for the frequency is in general smaller for the learned controllers than for the LQR controllers. On the other hand, the ℓ_2 norm of the control action is higher than in the LQR case.

Controllers' comparison for time-varying inertia

We evaluate the performance of different controllers in a simulation of the hybrid system switching among different inertia modes. We assume that the system starts in mode $q_2 = 0.5$s, and possible transitions of inertia can occur every 4 time steps. Figure 3.3 depicts the evolution of frequency deviation in node 1, under 5 different controllers for an initial condition $f_0 = -0.15$ Hz at every node. The controllers we use are the following: In blue, the frequency is controlled using the learned controller K_{L}. In red, we show the learned and virtual inertia controller $K_{\mathrm{L}} + \mathrm{VI}$ (ensure stability). Similarly, cyan depicts a controller that uses K_{L} and virtual inertia only when the system is in the unstable mode q_1. In black and green we use the optimal controllers K_q obtained from (3.6) for modes $q_3 = 1$s and $q_8 = 5$s, respectively. Around 4 seconds of the simulation, the system enters mode q_1 for around 0.4 seconds. This provokes an instability for controllers K_8 and K_{L}. After leaving the unstable mode the frequency is stabilized again. The other controllers are able to maintain stability in all the modes. In addition, key differences can be observed at the beginning of the simulation. Controller K_3 shows the highest overshoot of the simulation, while controller $K_{\mathrm{L}} + \mathrm{VI}$ (in red) is the fastest to peak due to the usage of the derivative of the frequency.

Table 3.2: Comparison of learned controller (K_L) and learned controller with virtual inertia ($K_\mathrm{L} + \mathrm{VI}$) against optimal control from LQR under different inertia modes. Units are in percentages (%).

Metric	q_1	q_2	q_3	q_4	q_5	q_6	q_7	q_8	q_9	q_{10}
$\|\|f_{K_\mathrm{L}}\|\|_\infty$	Unstable	-21.1	-10.4	-5.4	-1.1	2.6	5.9	8.8	11.9	14.4
$\|\|f_{K_\mathrm{L}+\mathrm{VI}}\|\|_\infty$	106.7	-16.1	-8.8	-4.3	-0.2	3.5	6.5	9.5	12.4	14.4
$\|\|f_{K_\mathrm{L}}\|\|_2$	Unstable	-9.0	-7.1	-5.5	-3.9	-2.5	-1.1	0.2	3.7	11.2
$\|\|f_{K_\mathrm{L}+\mathrm{VI}}\|\|_2$	**-7.2**	**-8.9**	**-7.4**	**-5.8**	**-4.3**	**-2.9**	**-1.5**	**-0.3**	**3.2**	**10.9**
$\|\|u_{K_\mathrm{L}}\|\|_\infty$	Unstable	3.2	-2.7	-5.9	-8.2	-10.2	-11.9	-13.3	-17.1	-15.2
$\|\|u_{K_\mathrm{L}+\mathrm{VI}}\|\|_\infty$	87.9	3.2	-2.7	-5.9	-8.2	-10.2	-11.9	-13.3	-17.1	-15.2
$\|\|u_{K_\mathrm{L}}\|\|_1$	Unstable	13.3	6.2	2.5	-0.3	-2.7	-4.7	-6.5	-11.0	-19.7
$\|\|u_{K_\mathrm{L}+\mathrm{VI}}\|\|_1$	78.1	19.0	8.6	4.2	1.1	-1.4	-3.6	-5.5	-10.2	-19.1
$\|\|u_{K_\mathrm{L}}\|\|_2$	Unstable	12.2	6.0	4.6	4.4	4.6	4.9	5.3	6.5	9.2
$\|\|u_{K_\mathrm{L}+\mathrm{VI}}\|\|_2$	45.2	16.4	8.7	6.6	5.9	5.8	5.9	6.1	7.1	9.4
J_{K_L}	Unstable	29.8	39.9	49.2	57.8	65.7	73.2	80.2	98.9	138.1
$J_{K_\mathrm{L}+\mathrm{VI}}$	39.1	31.6	40.2	49.0	57.4	65.3	72.6	79.5	98.1	137.3

Finally, the frequency for the first and third case (in blue and cyan) are almost identical except when the system is in the mode q_1. This shows that if we can detect when the system is in critical modes, we can apply virtual inertia control only when it is necessary to obtain a better performance.

3.4 Conclusions

In this work we propose a new framework for obtaining a constant data-driven controller for uncertain and time-varying power system dynamics. This is relevant because it can be intractable to solve frequency dynamics in real time (time-varying LQR) in large power networks. In addition, time-varying controllers, as the one from LQR, rely in the ability to predict or identify the current mode of the hybrid system. Finally, given the existing infrastructure and droop control, it would be simpler to implement a proportional controller with fixed gains compared to a time-varying control.

We use a switched affine hybrid system, where its modes change based on the changes of inertia in the system [8], we find optimal controllers using an LQR formulation. We use the solution (x, u) from the LQR as a dataset to train a fixed controller. We test our learned controller in different modes against optimal controllers. Results show that our learned controller can be used to obtain a similar performance as the optimal LQR controllers in the different modes. Finally, we show that adding a virtual inertia controller can stabilize the system for low inertia modes. This highlights the importance of using more flexible controllers when considering temporal variability in the system dynamics. For future work
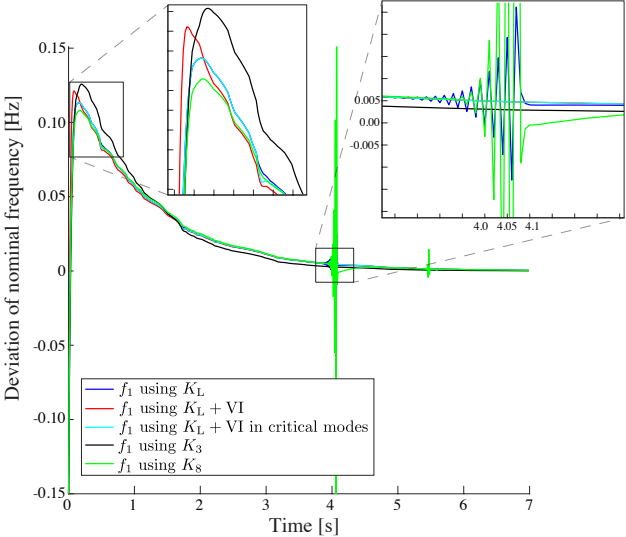
Figure 3.3: Frequency deviations for node 1 for 5 different controllers from a hybrid system simulation.

we plan to explore the performance of our controller with AC power flow, voltage dynamics, machine dynamics and power electronics (inverters) approximate dynamics. We will also compare our proposed controller with a robust controller. We also plan to study different learning algorithms with new features to test the efficiency of the learned controller, in particular promoting sparsity and information requirements using LASSO or Block Sparse Regression.

Bibliography

[1]   Hassan Bevrani, Toshifumi Ise, and Yushi Miura. "Virtual synchronous generators: A survey and new perspectives". In: *International Journal of Electrical Power & Energy Systems* 54 (2014), pp. 244–254.

[2]   Francesco Borrelli, Alberto Bemporad, and Manfred Morari. "Predictive Control for Linear and Hybrid Systems". In: *Cambridge University Press* (2017).

[3]   T. S. Borsche, T. Liu, and D. J. Hill. "Effects of rotational Inertia on power system damping and frequency transients". In: *Decision and Control (CDC), 2015 54th IEEE Conference on*. IEEE. Dec. 2015, pp. 5940–5946. DOI: 10.1109/CDC.2015.7403153.

[4]   E. Ela, M. Milligan, and B. Kirby. "Operating reserves and variable generation". In: *Nat. Renew. Energy Lab., Golden, CO, USA* (Aug. 2011).

[5]   Electricity Reliability Council of Texas (ERCOT). "Future Ancillary Services in ERCOT". In: *ERCOT: Taylor, TX, USA* (2013).

[6]   Michael Grant and Stephen Boyd. *CVX: Matlab Software for Disciplined Convex Programming, version 2.1*. http://cvxr.com/cvx. Mar. 2014.

[7]   Michael Grant and Stephen Boyd. "Graph implementations for nonsmooth convex programs". In: *Recent Advances in Learning and Control*. Ed. by V. Blondel, S. Boyd, and H. Kimura. Lecture Notes in Control and Information Sciences. Springer-Verlag Limited, 2008, pp. 95–110.

[8]   P. Hidalgo-Gonzalez et al. "Frequency Regulation in Hybrid Power Dynamics with Variable and Low Inertia due to Renewable Energy". In: *2018 IEEE Conference on Decision and Control (CDC)*. Dec. 2018, pp. 1592–1597.

[9]   Patricia Hidalgo-Gonzalez et al. "Frequency Regulation using Data-Driven Controllers in Power Grids with Variable Inertia due to Renewable Energy". In: *IEEE PES General Meeting*. IEEE. Aug. 2019.

[10]   P. Kundur. "Power System Stability and Control". In: *McGraw-Hill* (1994).

[11]   J. Löfberg. "YALMIP : A Toolbox for Modeling and Optimization in MATLAB". In: *In Proceedings of the CACSD Conference*. Taipei, Taiwan, 2004.

[12] E. Mallada. "iDroop: A Dynamic Droop controller to decouple power grid's steady-state and dynamic performance". In: *2016 IEEE 55th Conference on Decision and Control (CDC)*. Dec. 2016, pp. 4957–4964. DOI: `10.1109/CDC.2016.7799027`.

[13] Jos Notenboom et al. *Climate and Energy Roadmaps towards 2050 in north-western Europe: A concise overview of long-term climate and energy policies in Belgium, Denmark, France, Germany, the Netherlands and the United Kingdom.* Tech. rep. Netherlands: PBL Netherlands Environmental Assessment Agency, 2012.

[14] Bala Kameshwar Poolla, Saverio Bolognani, and Florian Dörfler. "Optimal placement of virtual inertia in power grids". In: *IEEE Transactions on Automatic Control* 62.12 (2017), pp. 6209–6220.

[15] Ujjwol Tamrakar et al. "Virtual inertia: Current trends and future directions". In: *Applied Sciences* 7.7 (2017), p. 654.

[16] Andreas Ulbig, Theodor S Borsche, and Göran Andersson. "Impact of low rotational inertia on power system stability and operation". In: *IFAC Proceedings Volumes* 47.3 (2014), pp. 7290–7297.

[17] Andreas Ulbig et al. "Predictive control for real-time frequency regulation and rotational inertia provision in power systems". In: *Decision and Control (CDC), 2013 IEEE 52nd Annual Conference on.* IEEE. 2013, pp. 2946–2953.

[18] Max Wei et al. "California's carbon challenge: Scenarios for achieving 80% emissions reductions in 2050". In: *Lawrence Berkeley National Laboratory, UC Berkeley, UC Davis, and Itron to the California Energy Commission* (2012).

[19] Qing-Chang Zhong and George Weiss. "Synchronverters: Inverters that mimic synchronous generators". In: *IEEE Transactions on Industrial Electronics* 58.4 (2011), pp. 1259–1267.